The Burble Effect: Superstructure and Flight Deck Effects on Carrier Air Wake

BRADLEY E. CHERRY[1] AND MATTHEW M. CONSTANTINO[2]
United States Naval Academy, Annapolis, MD, 21412

The purpose of the present work was to qualitatively and quantitatively model the air wake created by an aircraft carrier flight deck and superstructure in order to understand how it affects aircraft on approach and landing. The "burble effect" is the name given by navy pilots to the velocity deficit and downwash field immediately aft of an aircraft carrier. This turbulent region of air has adverse effects on landing aircraft and can cause pilots to bolter, missing the arresting wires and requiring another landing attempt. The experimental approach involved using a five-hole Pitot probe rake system for mapping of the air wake of a 6 ft aircraft carrier model. Wind tunnel tests were performed at Reynolds numbers of 11,000,000 and wake maps of 288 point measurements each were generated for configurations with and without the superstructure. The experiment showed that the superstructure created a region of extremely low flow velocity and downward flow angle. While the hull/deck configuration produced velocity deficits as low as 17%, the presence of the superstructure increased this to almost 30%. Furthermore, the addition of the superstructure decreased the downwash angle at the deck edge from -5 to -8 deg. Under these conditions, an aircraft on approach will experience an increased descent rate as it passes through the burble region. The presence of strong downwash compounds this adverse effect, making it more severe closer to the flight deck. Results also show that the superstructure geometry affects the severity of the burble effect.

Nomenclature

C	=	cone pressure calibration constant
C_L	=	lift coefficient
C_p	=	pressure coefficient
$C_{P_{23}}$	=	pitch pressure coefficient
$C_{P_{45}}$	=	yaw pressure coefficient
K_α	=	pitch flow angle calibration constant
K_β	=	yaw flow angle calibration constant
$\overline{p_c}$	=	average cone pressure
p_2	=	top pitch cone pressure
p_3	=	bottom pitch cone pressure
p_4	=	left yaw cone pressure
p_5	=	right yaw cone pressure
p_S	=	static pressure
p_T	=	total pressure
q	=	dynamic pressure
$\Delta\alpha$	=	flow pitch angle
$\Delta\beta$	=	flow yaw angle

[1] Midshipman 1/C, Aerospace Engineering Department, United States Naval Academy
[2] Midshipman 1/C, Aerospace Engineering Department, United States Naval Academy

Report Documentation Page

Form Approved
OMB No. 0704-0188

1. REPORT DATE	2. REPORT TYPE	3. DATES COVERED
2010		**00-00-2010 to 00-00-2010**

4. TITLE AND SUBTITLE	5a. CONTRACT NUMBER
The Burble Effect: Superstructure and Flight Deck Effects on Carrier Air Wake	5b. GRANT NUMBER
	5c. PROGRAM ELEMENT NUMBER
6. AUTHOR(S)	5d. PROJECT NUMBER
	5e. TASK NUMBER
	5f. WORK UNIT NUMBER
7. PERFORMING ORGANIZATION NAME(S) AND ADDRESS(ES) **United States Naval Academy,Annapolis,MD,21412**	8. PERFORMING ORGANIZATION REPORT NUMBER
9. SPONSORING/MONITORING AGENCY NAME(S) AND ADDRESS(ES)	10. SPONSOR/MONITOR'S ACRONYM(S)
	11. SPONSOR/MONITOR'S REPORT NUMBER(S)

12. DISTRIBUTION/AVAILABILITY STATEMENT
Approved for public release; distribution unlimited

13. SUPPLEMENTARY NOTES
American Society of Naval Engineers Launch & Recovery Symposium 2010, "Launch, Recovery & Operations of Manned and Unmanned Vehicles from Marine Platforms", December 8-9, 2010 Arlington, VA

14. ABSTRACT

15. SUBJECT TERMS

16. SECURITY CLASSIFICATION OF:			17. LIMITATION OF ABSTRACT	18. NUMBER OF PAGES	19a. NAME OF RESPONSIBLE PERSON
a. REPORT **unclassified**	b. ABSTRACT **unclassified**	c. THIS PAGE **unclassified**	**Same as Report (SAR)**	**15**	

I. Introduction

THE superstructure and deck/hull features of an aircraft carrier are known to generate turbulent airflow behind the carrier. This region of turbulent air has become known as "the burble," and it is often encountered by pilots immediately before landing. The burble causes planes to drop slightly, thus requiring a small amount of power to be temporarily added to maintain the glide slope though this region. The region is characterized by a downwards suction in the airflow and it is created by "the interference of the structure of the ship with the relative wind and its influence is felt mainly in the last half mile of the approach to the ship" [1]. Additionally, sea state, crosswinds, and features such as raised jet blast deflectors and flight deck traffic contribute to the burble.

The burble can be extremely dangerous to the unsuspecting pilot because it combines two separate, but equally hazardous, components. Aircraft approaching a carrier are on the verge of a stall due to the low speed and high angle of attack required by the approach, so when the aircraft pass through this region of lower air velocity produced by the superstructure wake, the lift over the wings is reduced, thus causing the aircraft to experience an increased descent rate. In addition to this negative effect, the aircraft also fly through a region where the flow is moving downward toward the water, typically 3 to 6 fps [2]. This region of downward flow coincides with the region of lower flow velocity caused by the superstructure; therefore, the two effects combine to produce the sinking effect of the "burble" that pilots describe.

The purpose of this experiment was to investigate the region of turbulent flow behind a 6 ft long representative aircraft carrier model with both the superstructure attached and removed at a Reynolds number of 11,000,000. The authors measured the velocity distribution and flow angularity of one vertical plane of the wake located at one-third of the carrier length aft of the model. Previous research has shown that the superstructure creates a region of extremely low flow velocity and a downward flow angle and this experiment was expected to validate those results [3].

The air wakes of ships which deploy aircraft have been the subject of numerous research programs, with the central focus to quantify the flowfield along the aircraft approach paths. Previous research has shown that subtle changes and protuberances in hull/deck/superstructure can have significant changes in the external flow characteristics and that these flow features can be severe [4,5]. This has been shown for DDG, LHA, and CV ship classes. For the aircraft carrier (CV), the flow pattern is primarily characterized by the formation of free vortices. One of these can appear along the leeward side of the hull [5] while others form at sharp edges of the deck-edge and superstructure. Cut-outs in the deck or sharp corners on the superstructure in general trap standing vortices which stabilize the wake structure in general and create a flowfield that is largely independent of the Reynolds number [6]. The fact that the overhang of the deck is a major cause for flow disturbance was experimentally validated by Lehman on a Forrestal-class carrier [7]. Durand and Wasicko also studied the effects of upwash and downwash on the glide path control of the approaching aircraft [8]. More recently, the burble was modeled in CFD by Polsky and Naylor. They found that the geometry of the stern had a significant impact on the airwake qualities along the aircraft approach path [3]. Other researchers have concentrated on the dynamic flowfield effects on the aircraft/ship coupling [9].

II. Experimental Setup and Procedure

A. Instrumentation

Closed-Circuit Wind Tunnel: Testing was done in the (CCWT) at the United States Naval Academy (USNA). The CCWT is single return wind tunnel with two ten inch diameter vents near the test section to equalize the static pressure. The test section is 60 inches in height, 40 inches in width, and 120 inches in length. Fillets run along the test section corners and gradually increase the cross sectional area to compensate for boundary layer growth to minimize the effects of horizontal buoyancy. The tunnel has a maximum flow rate of 295,000 cfm, a maximum Reynolds number of 1.9×10^6 per ft, and a maximum velocity of 300 feet per second (fps).

Wake-Interactive Survey Probe (WISP): The WISP is a custom-built automated data collection system that serves to capture a grid of flow measurements across a plane of the test section to produce "snapshots" of a flow. A 5 port Pitot-tube was used to record the dynamic pressure and flow angularity during testing. The tube has one port at the tip of its nose cone and four ports evenly spaced along the tip's conical sides.

A 5-hole probe is a useful tool for deducing flow angularity from pressure distribution. As seen in face-on view in Figure 1, the probe has one central port and four along the angled sides of the probe's tip. The flow pitch can be acquired with ports 2 and 3, the flow yaw can be acquired from ports 4 and 5, and the total pressure can be measured

with the central port. Equations 1, 2, and 3 are used to solve for the pressure coefficients. Equations 4 and 5, in conjunction with calibration values from Table 1, are used to find for the flow pitch and yaw angles [10].

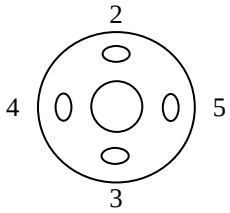

Figure 1. Upright 5-Hole Probe

Table 1. Calibration Constants for the 5-Port Probes

	Probe 1	Probe 2	Probe 3
K_α	34.686	35.137	35.273
K_β	32.195	32.669	32.712
C	0.923	0.936	0.935

$$\overline{p_c} = \frac{p_2 + p_3 + p_4 + p_5}{4} \tag{1}$$

$$C_{P_{23}} = \frac{p_2 - p_3}{p_T - \overline{p_c}} \tag{2}$$

$$C_{P_{45}} = \frac{p_4 - p_5}{p_T - \overline{p_c}} \tag{3}$$

$$\Delta\alpha = K_a C_{P_{23}} \tag{4}$$

$$\Delta\beta = K_b C_{P_{45}} \tag{5}$$

Using the 5-hole probe, it is possible to determine the velocity magnitude. Equation 6 below is derived from Bernoulli's equation, which says that the total pressure along a streamline is constant, provided the flow is steady. However, the static pressure provided from the 5-hole probe is not the true static pressure and must undergo a calibration. The values for C, like K_α and K_β, are unique for each probe, and are included in Table 1.

$$V = \sqrt{\frac{2 \cdot q}{\rho}} = \sqrt{\frac{2 \cdot (p_T - p_S)}{\rho}} \approx \sqrt{\frac{2 \cdot \left((p_T - \overline{p}_c)/C\right)}{\rho}} \tag{6}$$

The 5 port Pitot-tube was installed on an adjustable arm that extended out through a thin slit of the test section wall. The arm was mounted to two coupled Newport precision motion linear stages secured to a lab bench bolted to the lab deck floor. The linear stages were controlled via a Matlab GUI which was capable of moving the probe across any user-specified grid of points. The mounting system included features to minimize vibration and interference with test section flow. The WISP allowed data to be continuously recorded as the wind tunnel ran without the need to manually adjust the position of the probe.

PSI Inc. System 8400 Pressure Instrumentation: The Pressure Systems, Incorporated (PSI) System 8400 was the primary instrument for collecting data. The system consists of the main frame linked to electronically-scanned pressure (ESP) modules that are each able to acquire data from 16, 32, or 48 ports. The ESP modules read gauge pressure, referenced to the atmospheric pressure determined by the Pressure Standard Unit (PSU) that is within ±0.02% FS accuracy. The pressure differential is measured by the ESP module using an array of piezoresistive pressure sensors mounted on a hybrid glass substrate. A slight deflection of the crystal structure of the sensor considerably alters its resistive properties and allows sensitive measurements to be made.

Carrier Model: The model used in this experiment was a 6 ft long simplified version of the CVN 71 USS Theodore Roosevelt with a detachable superstructure built by the USNA Machine Shop and is shown in Figure 2. The superstructure was represented with three stacked blocks for the base, bridge and observation decks, and

antenna mast. The model was mounted at a 9 deg yaw in the test section in order to orient the angled runway straight into the wind, as is standard practice for US Navy aircraft carriers conducting aircraft recovery operations.

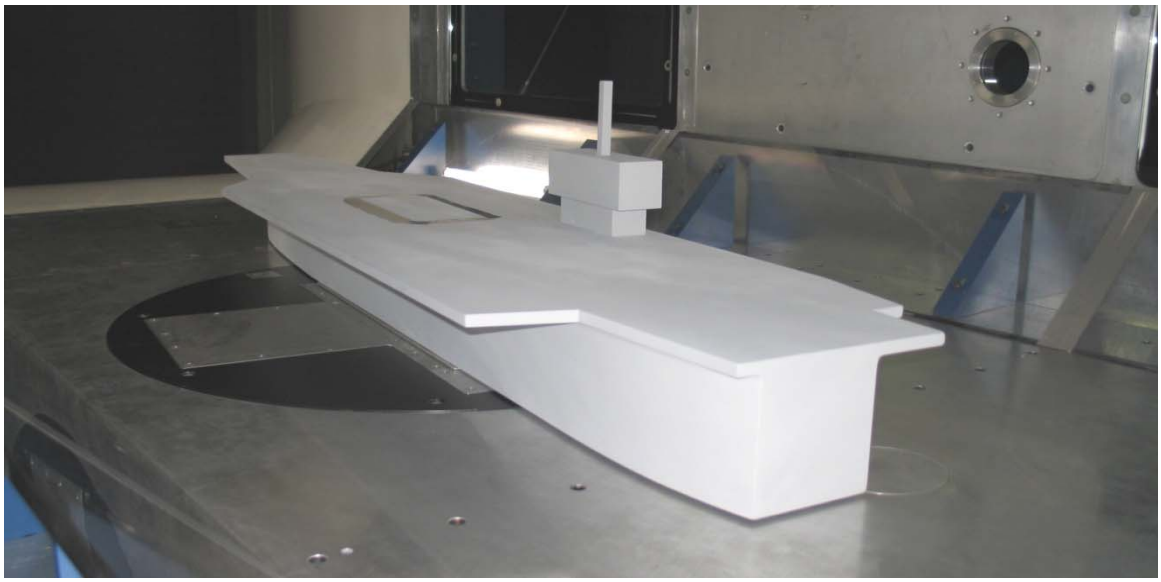

Figure 2. Carrier Model

Superstructure Models and Fillets: Two representative superstructure models for the Nimitz and Ford Class carriers are shown below in Figure 3 and Figure 4. The models were installed on the model aircraft carrier's deck in their actual locations according to top view deck plans. Compared to the Nimitz class model, the Ford class model is located further aft and outboard from the centerline.

Figure 3. CVN-68 Nimitz Class Superstructure & Model

Figure 4. CVN-78 Ford Class Superstructure & Model

A second feature that was investigated was deck fillets. Removable fillets were built to install in the two notches in the back of the deck. Increasing the deck space can be useful for taxiing aircraft and parking them on deck, therefore the effects of how rounding out the corners of the aircraft carrier's deck would influence the burble was investigated. Figure 5 shows the two fillets and it is noted the fillet on the starboard side is the small fillet.

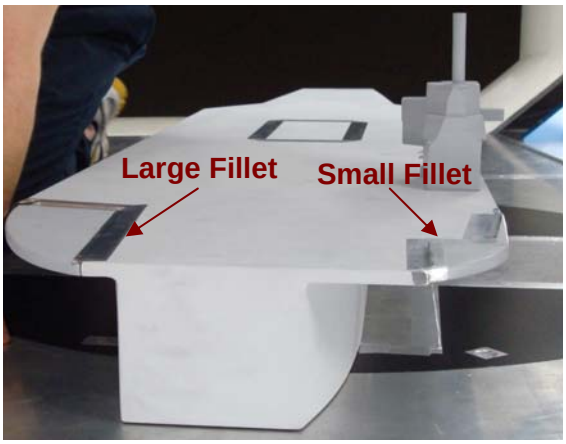

Figure 5. Flight Deck With Large and Small Fillets

Procedure

This experiment was conducted on 18 April 2009 and Table 2 shows the different combinations of variables used for the following tests. Configuration 1 is most representative of the current CVN-68 Nimitz class aircraft carrier and Configuration 3 is most representative of the future CVN-78 Ford class aircraft carrier. The PSI System 8400 was first calibrated using a nitrogen gas cylinder at 130 psia. The window of locations to survey by the probe and the measurement intervals were input into the WISP GUI. Dynamic pressures were recorded using the 5 port Pitot-tube after the test section flow was allowed to stabilize. A total of 288 data points were recorded for each survey.

Table 2. Test Configurations Descriptions

Configuration 1	Box SS + Small Fillet
Configuration 2	Box SS + Both Fillets
Configuration 3	Ford SS + Small Fillet
Configuration 4	Ford SS + Both Fillets

III. Results

In order to determine the effects caused by the superstructure and deck geometry on landing aircraft, the free stream velocity, velocity pitch angle (α), and the velocity yaw angle (β) were determined at a distance of 2 ft behind the carrier for the box superstructure, Ford superstructure, and for flight deck/superstructure configurations listed in Table 2. These results were then compared graphically.

The following figures show the air wake characteristics plotted on a coordinate system referenced to the balance center. The y-axis is the distance left or right of the balance center, the z-axis is the height above the test section floor, and the positive x-axis is in the direction of the downstream flow. Therefore the plots show one vertical slice of the wake at a distance of 2 ft aft of the aircraft carrier model, corresponding to 380 ft aft of a full-scale carrier, or the distance where a landing aircraft is located 1.3 s before touchdown. Also, using a glide slope of 3.5°, the position of the aircraft at 2 ft behind the carrier is found to be about 7 inches above the test section floor [8].

A. Ford Class Superstructure vs. Box Superstructure

A.1. Flow Velocity

Figure 6 and Figure 7 show the velocity magnitude at a location two feet behind the stern of the carrier model with the black outline representing the location of the carrier deck and superstructure relative to the plot area. In both Figure 6 and Figure 7, a region of low flow velocity is seen on the left side of the plots from about y=-15 inches to y=-8 inches and from z=4 inches to z=10 inches. This region is showing the effects of a vortex being generated by the shape of the flight deck and is unaffected by the geometry of the superstructure.

However, the superstructure geometry clearly affects the velocity magnitude footprint behind the carrier in the region from y=-5 inches to y=8 inches and z=3 inches to z=9 inches as shown by Figure 6 and Figure 7. In Figure 6, there is a large region of dark blue, indicating a region of low flow velocity. This area sees a velocity that is 26% lower than the free stream velocity of 310 fps; furthermore, the region of low flow velocity impinges on the approach path of landing aircraft. The approximate location of an aircraft on landing approach, y=-3 inches and z=7 inches, experiences a velocity that is 13% lower than the free stream velocity.

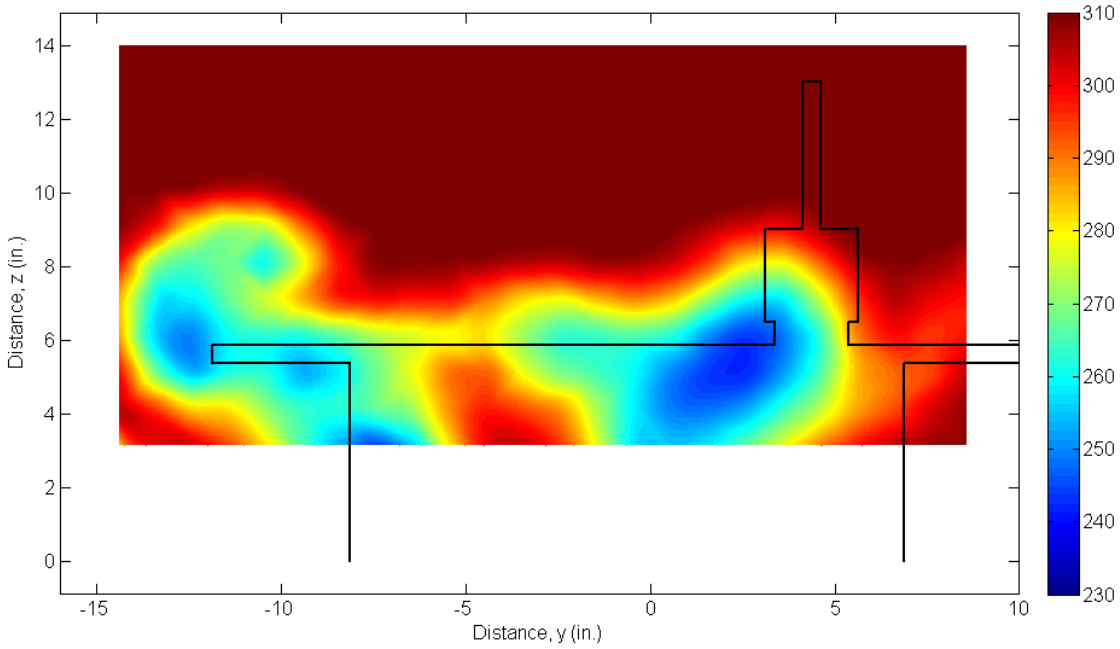

Figure 6. Flow Velocity Magnitude for Box Superstructure Configuration

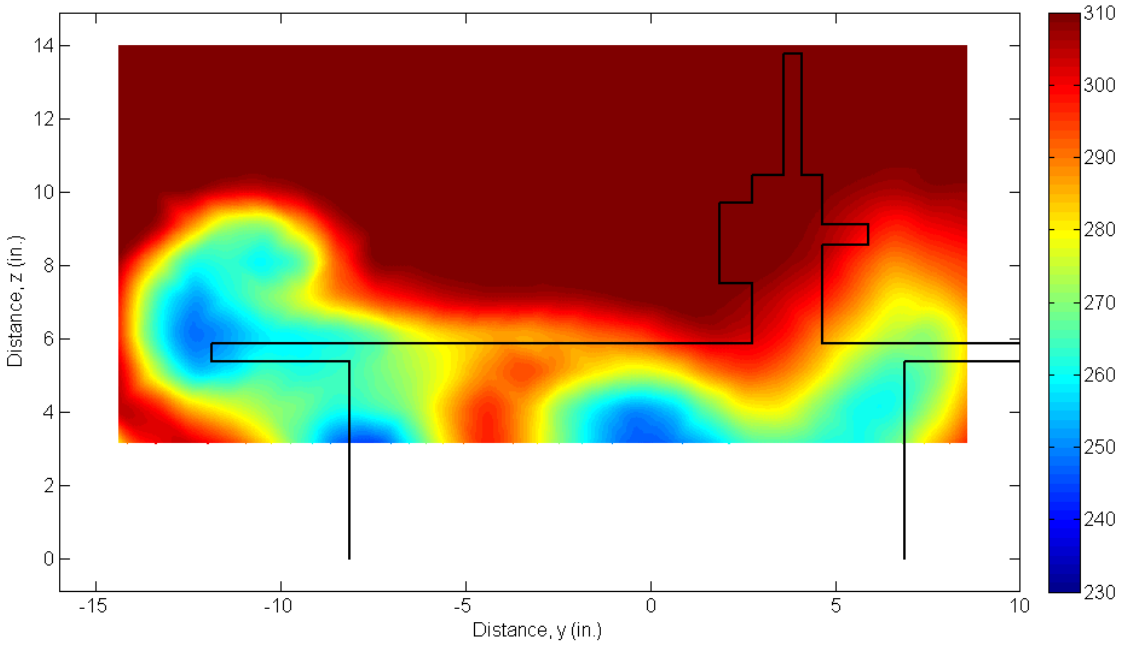

Figure 7. Flow Velocity Magnitude for Ford Superstructure Configuration

In Figure 7, the region of low flow velocity due to the superstructure is "shoved" downwards and to the right. The velocity magnitude in this region is also only 19% lower than free stream; therefore, the Ford superstructure's velocity drop is 7% less than the box superstructure. However, the most noticeable difference in the Ford superstructure is at the aircraft approach point of y=-3 inches and z=7 inches. At this location, the flow velocity is only 4% lower than the free stream velocity. This is an improvement of 9% compared to the box superstructure.

A.2. Flow Pitch Angle

Figure 8 and **Figure 9** (next page) show the distribution of the pitch flow angles behind the carrier. These plots reveal where the flow is traveling upwards or downwards and at how many degrees. The dark red indicates a high upwash, dark blue indicates high downwash, and the pale green indicates horizontal flow. It is important to note that once again the left half of the graph appears to be roughly the same for both configurations. The low flow velocity seen on the left half of the graph in Figure 6 and Figure 7 suggested the presence of a vortex, and the flow pitch angle graphs, Figure 8 and **Figure 9**, confirm that there is indeed a vortex created by the deck and hull of the carrier. The strong upwash at y=-13 inches, z=9 inches coupled with the downwash at y=-8 inches, z=9 inches suggest that a vortex is present in the flow. Since the test was only run at a location two feet behind the carrier, the results provide only one slice of the flow pattern behind the ship, thus only the portion of the vortex where it is beginning to rotate downward is shown. Also, the large dark blue area on the right side of both Figure 8 and **Figure 9** represents a region of high downwash. This downwash region is only slightly affected by superstructure geometry and shifts slightly downward and leftward for the Ford superstructure when compared to the box superstructure. However, it is important to note that this region is not in the approach path for landing aircraft; therefore, the superstructure effects in this region can be neglected.

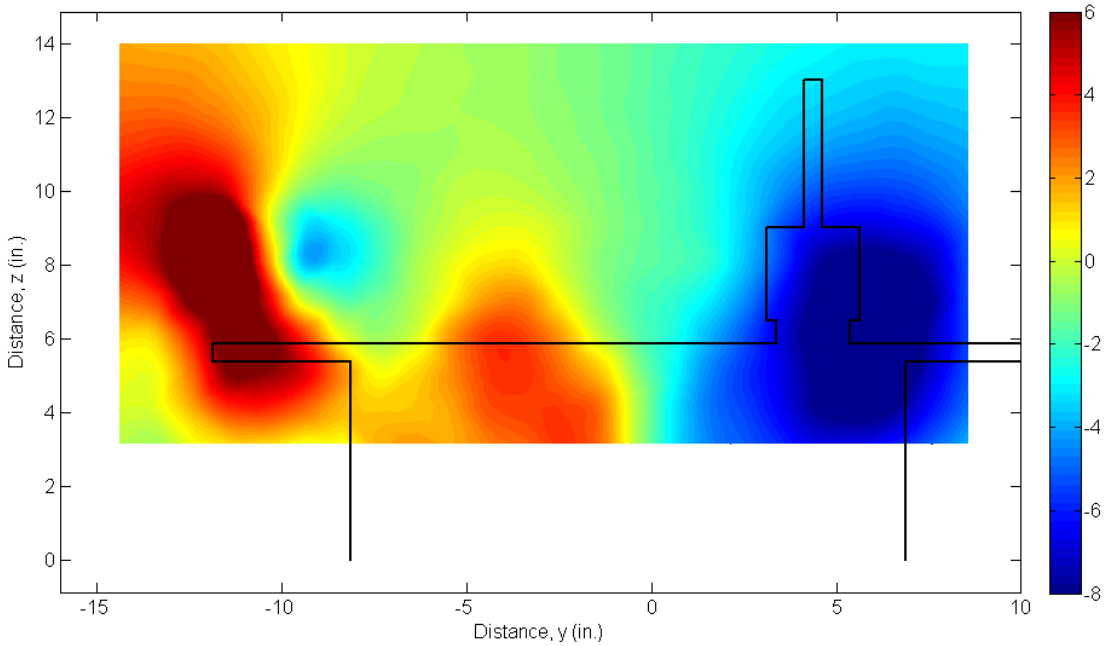

Figure 8. Flow Pitch Angle for Box Superstructure Configuration

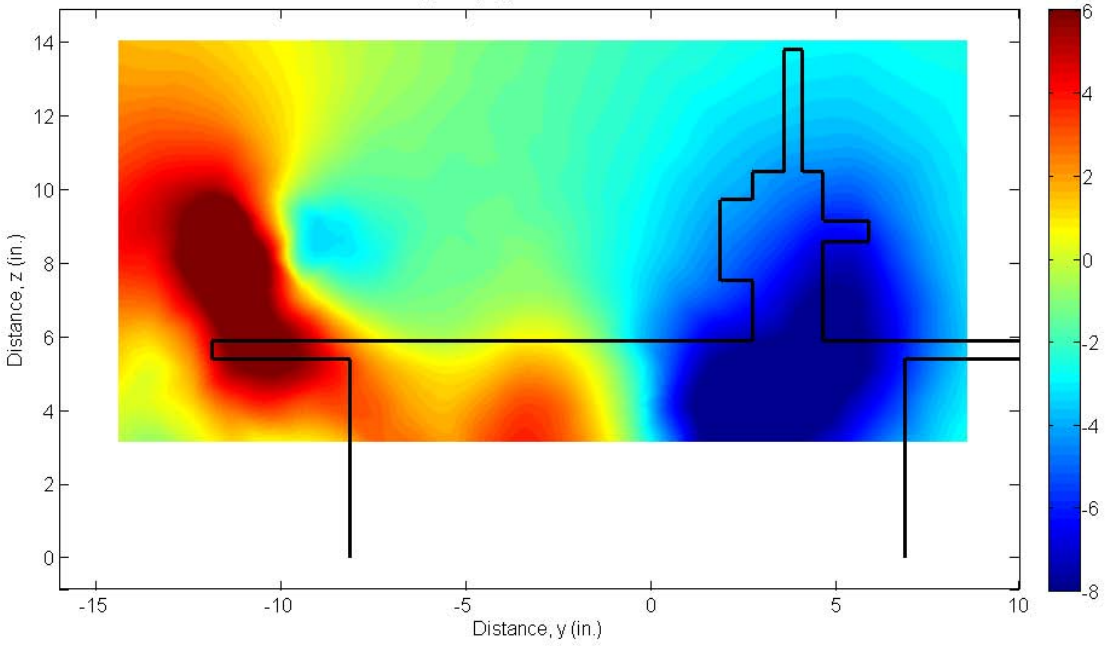

Figure 9. Flow Pitch Angle for Ford Superstructure Configuration

Conversely, in Figure 8, a large spike in upwards flow can be seen impinging on the approach and landing region for the box superstructure. This upwash spike causes there to be an upwards flow of +2 degrees at the aircraft approach point for the box superstructure. However, the Ford superstructure dramatically reduces the spike in upwash at this same location as shown by **Figure 9**. For the Ford superstructure, the upwash at the approach point is reduced to -0.5 degrees. Therefore, the Ford superstructure can be said to decrease the upwash in the approach region by 25% when compared to the box superstructure.

A.3. Flow Yaw Angle

The final flow aspect that causes the burble is the flow yaw angle. The flow yaw angle graphs are shown below for each configuration and are labeled Figure 10 and Figure 11. Dark red colors indicate positive yaw angles (to the right), dark blue colors indicate negative yaw angles (to the left), and light orange colors indicate a yaw angle of zero degrees.

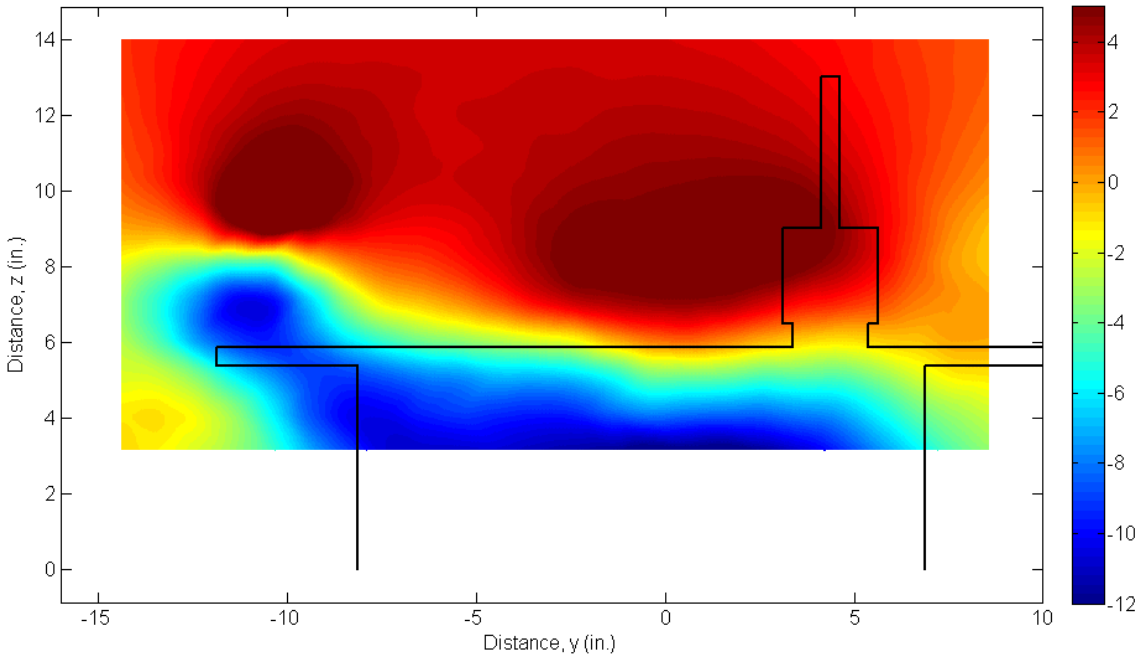

Figure 10. Flow Yaw Angle for Box Superstructure Configuration

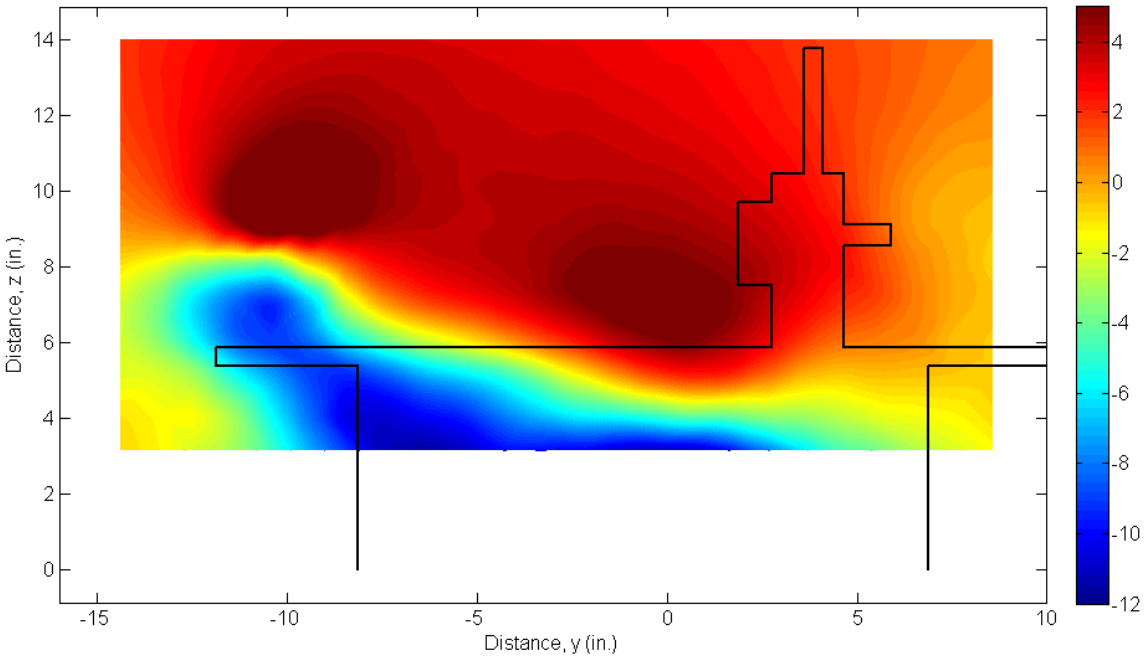

Figure 11. Flow Yaw Angle for Ford Superstructure Configuration

In both Figure 10 and Figure 11, the flow is seen to be moving to the left below the deck of the carrier, but this is to be expected and can be explained because the airflow is essentially "whipping" around the back of the carrier. However, all of the negative yaw angles that are beneath z=5.5 inches can be said to have no effect on landing aircraft because even in the most extreme of situations, an aircraft should never be that low behind the carrier. On another note, the flow is also negative for both Figure 10 and Figure 11 in the region of the vortex generated by the deck and hull, y=-15to y=-7 and z=4 to z=8. Also, the same vortex causes the flow to move to the right where y=-9 inches, z=9.5 inches for both configurations. These features appear almost the same on both figures; therefore, it can be said that the superstructure geometry has a minimal affect on the flow yaw angle in the landing region. At the aircraft approach point, y=-3 inches and z=7 inches, the flow has a yaw angle of about +1.3 degrees for the box superstructure (Figure 10) and a yaw angle of about +2.5 degrees for the Ford superstructure. This slight increase in positive yaw of 1.2 degrees does not affect the lift being produced by the aircraft's wings; therefore, it does not contribute to the increased sink rate that aircraft experience as they fly through the burble.

B. Intermediate Conclusions

The effects of superstructure geometry are summed up in the following table.

Table 3. Effects of superstructure geometry at approach point

	Free stream Velocity	pitch angle (α)	yaw angle (β)
Box SS	270 fps	2 deg	1.3 deg
Ford SS	298 fps	-0.5 deg	2.5 deg

Based on Table 3, it can be said that the geometry of the Ford superstructure will reduce the burble effect compared to the box superstructure for three main reasons. First, the Ford superstructure causes less of a free stream velocity decrease in the landing and approach regions. A higher free stream velocity means that the aircraft will produce more lift; therefore, aircraft on approach to the Ford will not experience as much of a drop when flying through the burble because the velocity seen by the wings of that aircraft will be higher than when approaching the older style box superstructure. Secondly, the Ford superstructure does not induce as high a flow pitch angle in the landing and approach regions. Typically, upwash would serve to increase the total lift of the wing by increasing the effective angle of attack, thus generating a higher value of C_L. However, approaching aircraft are already operating at high values of C_L due to their high angle of attack; therefore, an increase in C_L could result in a wing stall, thus causing the aircraft to momentarily drop. However, unlike the box superstructure, the Ford superstructure induces a negative flow pitch angle in the approach region. The downwards flow in this case would serve to lower the effective angle of attack, thus resulting in a smaller C_L value, and thus less lift. Therefore, because landing aircraft are at high C_L values and a high angle of attack, lift is lost as the aircraft comes through the burble regardless of whether the flow is an upwash or a downwash. However, because the flow pitch angle induced by the Ford superstructure in the approach region is nearly 0 degrees, an aircraft on approach to the Ford will not see as much of a sink rate increase when compared to flying the same approach on a carrier equipped with the older box superstructure. Finally, the Ford superstructure induces a slightly higher yaw angle in the approach region, but the flow yaw angle has a negligible effect on the ability of the aircraft to produce lift. Therefore, the flow yaw angle does not really contribute to the increased sink rate that characterizes the burble.

C. Flight Deck Geometry Effects for Ford Class

Further analysis was conducted in order to study the possible effects of the flight deck geometry on the burble. These tests were conducted for the configurations listed below in Table 4. It was found that the flight deck geometry mainly affected the port side of the flow field behind the carrier and was independent of the type of superstructure installed. Therefore, this section seeks to characterize the deck/hull vortex for the Ford class aircraft carrier, configurations 3 and 4. All measurements were taken in a vertical plane two feet behind the stern of the carrier model.

Table 4. Test Configurations Descriptions

Configuration 1	Box SS + Small Fillet
Configuration 2	Box SS + Both Fillets
Configuration 3	Ford SS + Small Fillet
Configuration 4	Ford SS + Both Fillets

C.1. Flow Velocity

The flow free stream velocity without the large fillet, configuration 3, is shown in Figure 12, and the flow free stream velocity with the large fillet, configuration 4, is shown in Figure 13.

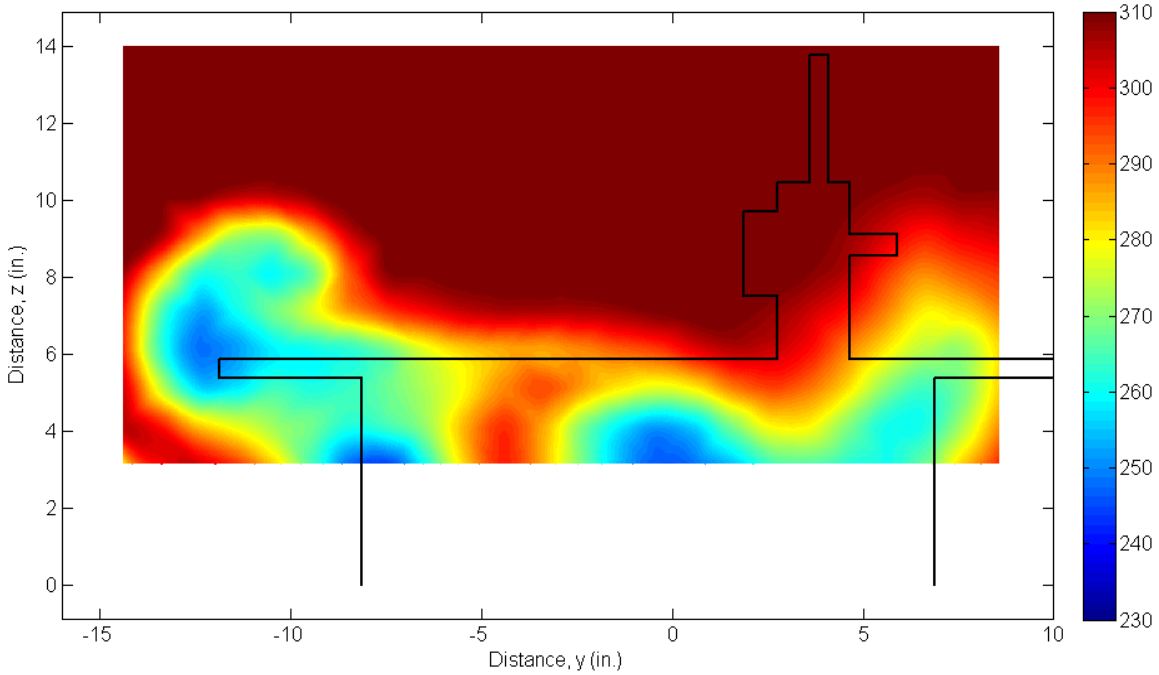

Figure 12. Flow field velocity for configuration 3 (Small Fillet Only)

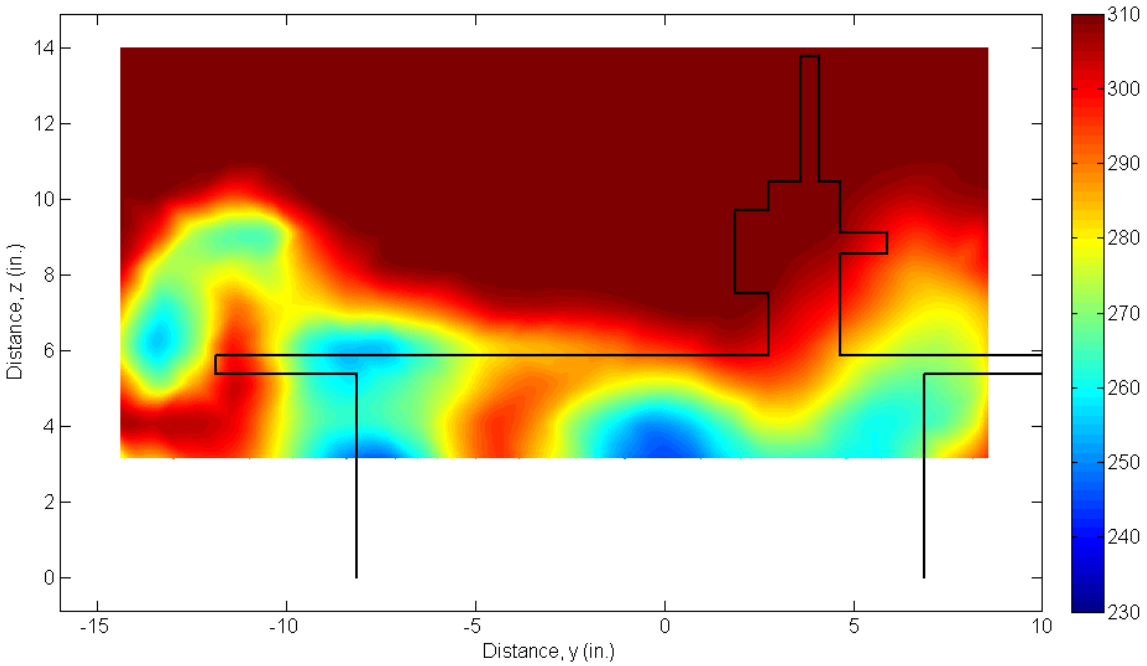

Figure 13. Flow field velocity for configuration 4 (Small + Large Fillet)

By comparing Figure 12 and Figure 13, it becomes obvious that the large fillet only affects the flow field on the port side of the carrier. By adding the large fillet to the "notch" on the aft, port side of the carrier, the intensity of the deck/hull vortex is greatly reduced as shown in Figure 13. The dark blue color that is centered on y=-12 inches and z=6 inches in Figure 12 denotes the core of the deck/hull vortex; however, in Figure 13 this area no longer exists. In general, the entire vortex shown in Figure 13 is less intense and causes less of a velocity deficit than the vortex shown in Figure 12.

C.2. Flow Pitch Angle

The flow pitch angle without the large fillet installed, configuration 3, is shown in Figure 14, and the flow pitch angle with the large fillet installed, configuration 4, is shown in Figure 15.

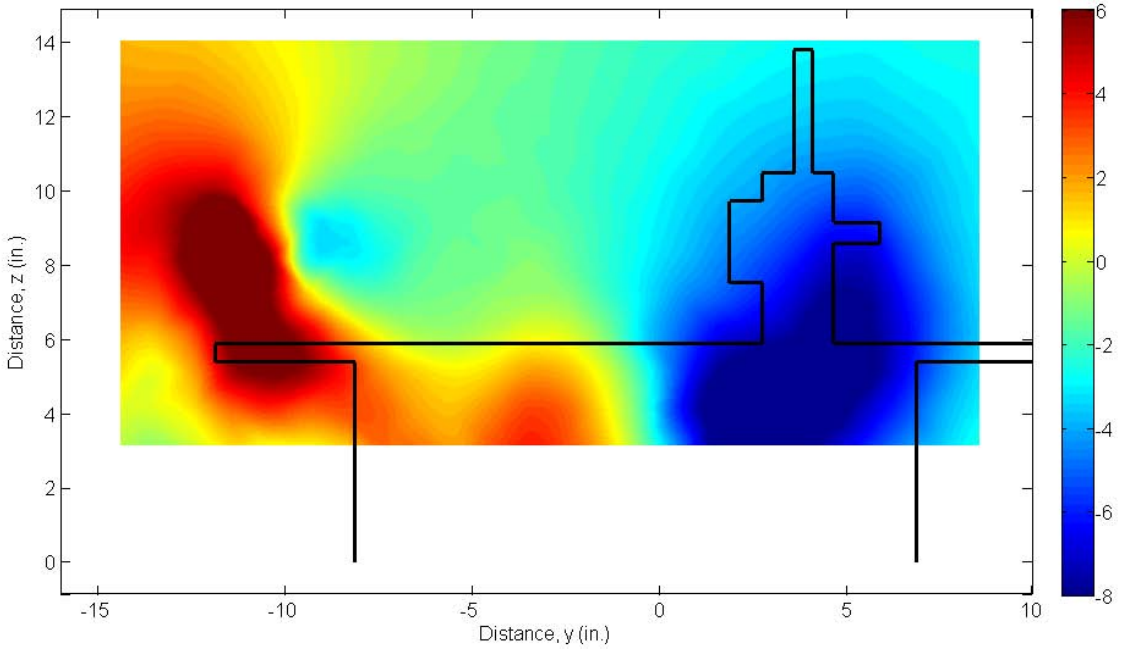

Figure 14. Flow pitch angle for configuration 3 (Small Fillet Only)

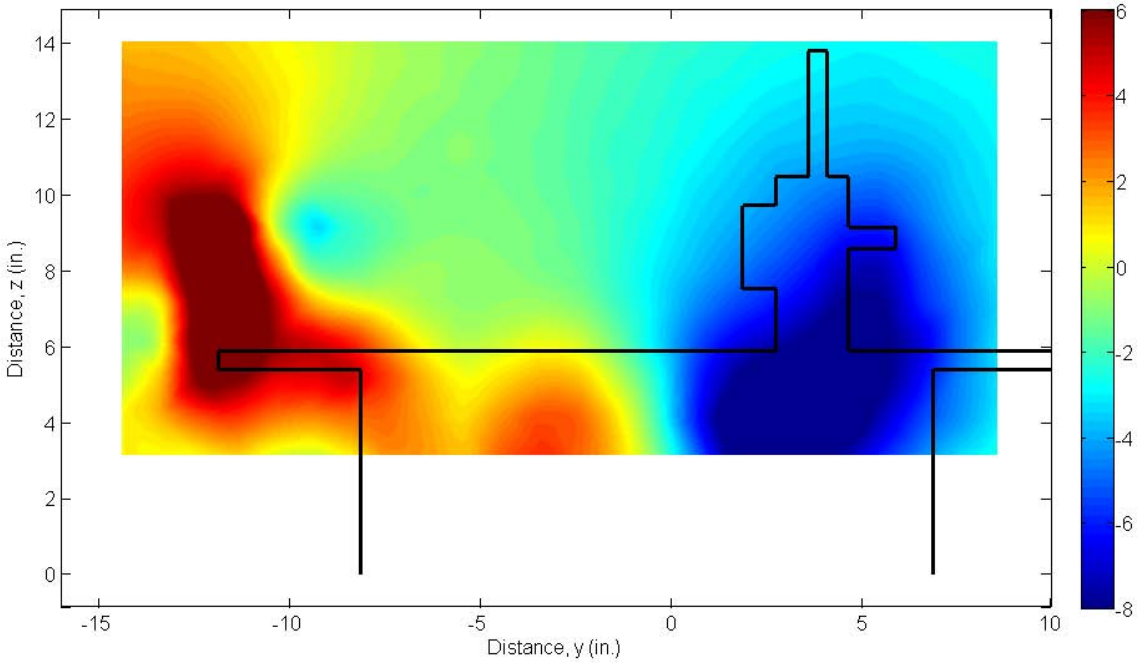

Figure 15. Flow pitch angle for configuration 4 (Small + Large Fillet)

The flow pitch angle does is not as drastically affected as the flow free stream velocity with the addition of the large fillet as shown above in Figure 14 and Figure 15. However, all that this proves is that a vortex still does exist with the addition of the large fillet, but as previously discussed the vortex is less intense once the fillet is added.

C.3. Flow Yaw Angle

Figure 16 and Figure 17, below, show the flow yaw angle for configuration 3 and configuration 4 respectively.

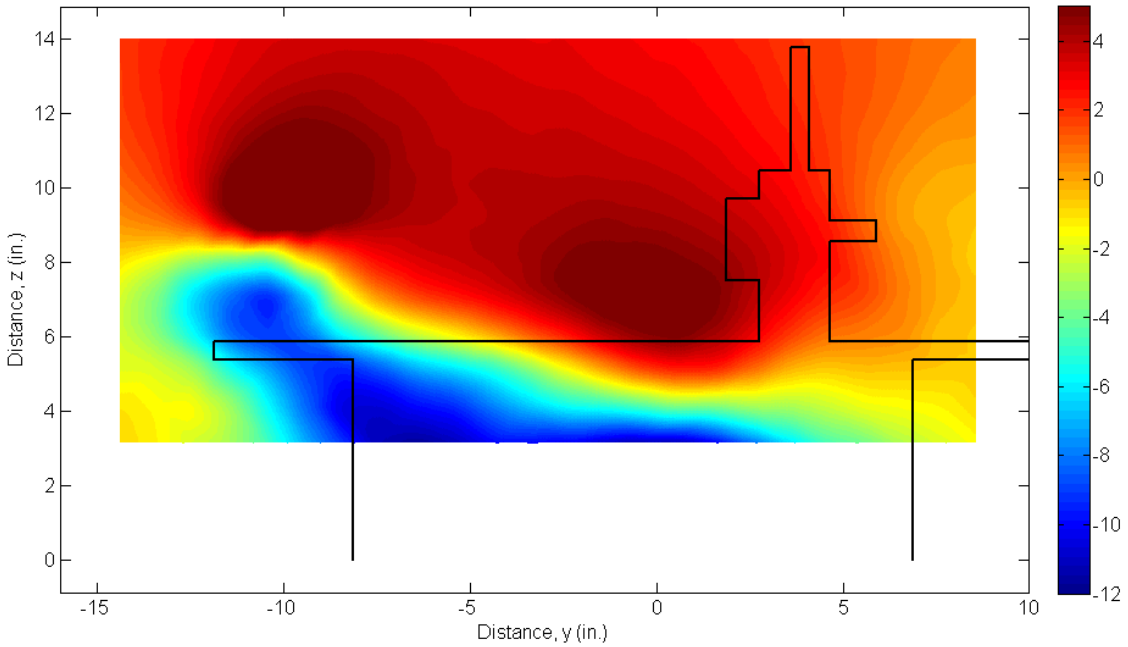

Figure 16. Flow yaw angle for configuration 3 (Small Fillet Only)

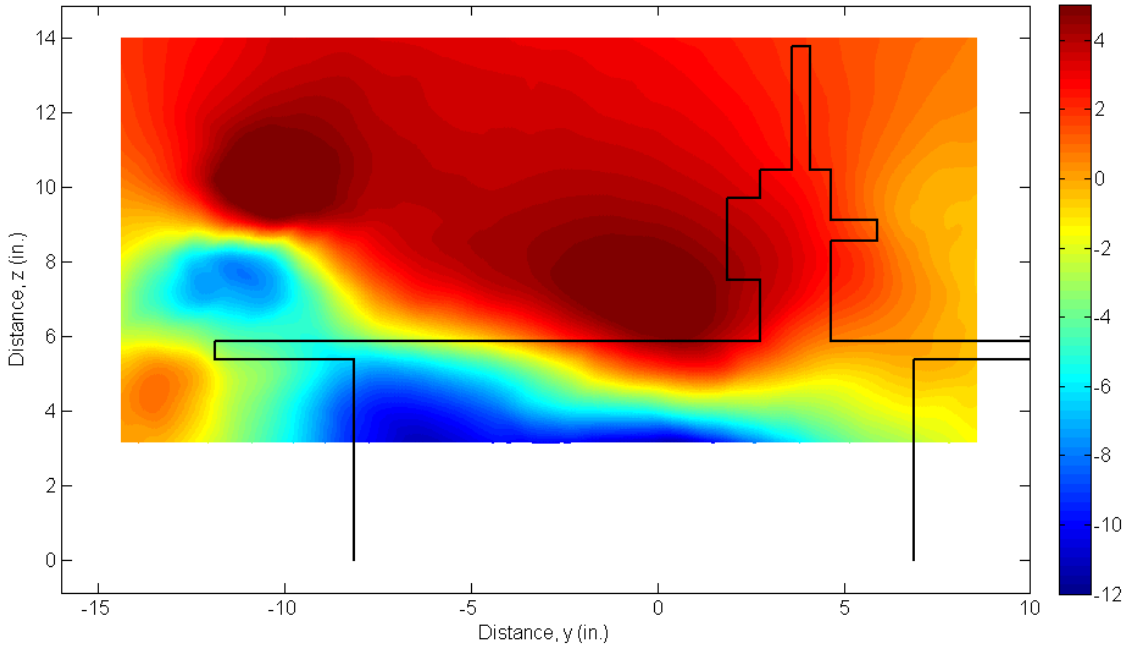

Figure 17. Flow yaw angle for configuration 4 (Small + Large Fillet)

The addition of the large fillet slightly reduces the leftward flow in the region surrounding y=-11 inches and z=7 inches. In Figure 16, the deck/hull vortex is moving toward the left at an angle of -10 degrees; however, in Figure 17, the deck/hull vortex is only moving toward the left at an angle of -7 degrees. Also, the area of leftward moving flow in Figure 17 is smaller in size than the same area in Figure 16. Once again, this shows that the deck/hull vortex is reduced by adding the large fillet.

D. Discussion/Conclusion

It is important to note that the study conducted on the effect of the fillets on the deck/hull vortex was conducted at a length of two feet behind the carrier. As previously stated, this length corresponds to distance of 380 feet aft of a real, full-scale carrier. Even at this distance, the vortex and burble appeared relatively intact. Due to equipment and wind tunnel mounting restraints, it was not possible to analyze the deck/hull vortex and burble effect immediately over and aft of the flight deck. The deck/hull vortex appears to be "sucked" upwards through the "notch" in the back of the carrier flight deck and subsequently rolls downstream behind the carrier. The addition of the large fillet drastically appears to reduce the intensity of the deck/hull vortex, even at a full-scale distance of 380 feet. Therefore, it would appear to be beneficial to fill in the "notch" in the back, port corner of the flight deck on aircraft carriers. Not only would this fillet reduce the deck/hull vortex and prevent it from rushing up and over the landing/approach area, but it would also provide room for aircraft and/or equipment storage.

The burble effect is caused by multiple factors such as free stream velocity deficits, upwash and downwash, and vortices that are generated from the superstructure and the deck/hull. All of these various aspects of the burble combine to produce the increased sink rate on approach that has been described by many carrier pilots. Additionally, an aircraft carrier's superstructure and flight deck geometry both contribute to the burble effect. Since Nimitz class carrier construction has ended and Ford class carrier construction has just begun, the potential exists for future carriers to be designed such that the burble effect becomes reduced.

Acknowledgments

The authors would like to thank the USNA Aerospace Engineering Department, the E&W Fluids Laboratory staff, the Technical Services Department, Mr. Dale Boyer, CAPT John Manvel USN (Ret.), and especially Professor Miklosovic.

References

[1]Rudowsky, T., Cook, S., Hynes, M., Heffley, R., Luter, M., Lawrence, T., Niewoehner, R., Bollman, D., Senn, P., Durham, W., Beaufrere, H., Yokell, M., Sonntag, A., "Review of the Carrier Approach Criteria For Carrier-Based Aircraft – Phase I; Final," Naval Air Warfare Center Aircraft Division., Rept. NAWCADPAX/TR-2002/71, Patuxent River, MD, Oct. 2002.

[2]"NATOPS Landing Signal Officer Manual," Naval Air Technical Data and Engineering Service Command, NAVAIR 00-80T-104, Naval Air Station, North Island, San Diego, CA 92135–7031, 2001.

[3]Polsky, S., and Naylor, S., "CVN Airwake Modeling and Integration: Initial Steps in the Creation and Implementation of a Virtual Burble for F-18 Carrier Landing Simulations," NAVAIR, Patuxent River, MD, 20670, 2005.

[4]Nixon W. B., "Preliminary Smoke Tunnel Study of Steady State Ship-Induced Turbulence of a Destroyer Model." Naval Air Engineering Center, NAEC-MISC-903-13, Lakehurst, NJ, 1978.

[5]Perelli, R. J., "Smoke Tunnel Study of a 1/200 Scale DD 963 Ship Model," NAEC-91-9030, Naval Air Engineering Center, Lakehurst, NJ, 1984.

[6]Hoover, C., "Carrier Airflow Analysis- Smoke Tunnel and Full Scale Comparison of CVA-61," NAEF-ENG-6776, US Naval Air Material Center, Philadelphia, PA, 1961.

[7]Lehman, A. F., "An Experimental Study of the Dynamic and Steady-State Flow Disturbances Encountered by Aircraft during a Carrier Landing Approach," *Journal of Aircraft*, Vol. 3, No. 3, 1966, pp. 208-212.

[8]Durand, T. S., and Wasicko, R. J., "Factors Influencing Glide Path Control in Carrier Landing," *Journal of Aircraft*, Vol. 4, No. 2, 1967, pp. 146-158.

[9]Shipman, J. D., Arunajatesan, S., Cavallo., P. A., Sinha, N., and Polsky., S. A., "Dynamic CFD Simulation of Aircraft Recovery to an Aircraft Carrier," Combustion Research and Flow Technology, Inc. (CRAFT Tech) and Naval Air Systems Command, Patuxent River, MD, 2008.

[10]Sink, E., "USNA Closed Circuit Wind Tunnel Flow Quality," United States Naval Academy, Annapolis, MD, 2008 (unpublished).